Production of e^+e^- in proton-lead collision: Photon-photon fusion

Barbara Linek,[1,*] Marta Łuszczak,[1,†] Wolfgang Schäfer,[2,‡] and Antoni Szczurek[2,§]

[1]*College of Natural Sciences, Institute of Physics, University of Rzeszów, ul. Pigonia 1, PL-35-959 Rzeszów, Poland*

[2]*Institute of Nuclear Physics, Polish Academy of Sciences, ul. Radzikowskiego 152, PL-31-342 Kraków, Poland*

(Received 30 August 2022; accepted 7 November 2022; published 28 November 2022)

We analyze the photon-initiated processes for production of e^+e^- pairs in proton-nucleus collisions at LHC energy, taking into account both elastic processes and proton dissociations in the low-mass region (LMR) and intermediate-mass region (IMR) as defined by the ALICE collaboration. The calculations are performed within the k_T-factorization approach, including transverse momenta of intermediate photons. We discuss several differential distributions in invariant mass of both the leptons M_{ll}, pair rapidity Y_{ll} and transverse momenta of the lepton pair $p_{t,ll}$. In addition, we present the two-dimensional distributions in $\log_{10} x_{Bj}$ and $\log_{10} Q^2$ and $(\log_{10} W, \log_{10} Q^2)$ the arguments of the deep-inelastic structure functions. All presented results were obtained with modern parametrizations of proton structure functions. Limiting to small invariant masses of dielectrons one tests structure functions in the nonperturbative region of small Q^2 and/or small W. We quantify difference for different parametrizations from the literature. We estimate gap survival factor and discuss experimental possibilities.

DOI: 10.1103/PhysRevD.106.094034

I. INTRODUCTION

There are many mechanisms of dilepton production in pp, pA, and AA collisions. In pp collisions these are Dalitz decays at low dilepton masses and semileptonic decays of mesons or Drell-Yan processes. There the gamma-gamma processes exist but the contribution is rather small. However, it can be measured by imposing rapidity gaps, see for example [1]. Until recently in nucleus-nucleus collision, the problem was separated into real hadronic collisions ($b < R_1 + R_2$), where the mechanism are similar as in proton-proton collisions and ultraperipheral collisions ($b > R_1 + R_2$), where the dominant mechanism is photon-photon fusion. It was, however, shown, (see, e.g., [2]) that the photon-photon processes survive also in the semicentral collisions and actually dominate at very small transverse momenta of the dilepton pair. In pA collisions the issue was not carefully analyzed. The only exception is [3]. The authors of the paper made a feasibility study for the ATLAS experimental apparatus. The recent ALICE measurements [4] on dilepton production in proton-lead collisions are the motivation for carrying out the present research.

Here we wish to thoroughly investigate the contribution of photon-initiated processes to the production of dileptons in proton-nucleus collisions, in order to determine the parameters enabling future measurements. Due to the fact that the nucleus in discussed collisions is only a source of "elastic" photons, there are only two types of photon-initiated dilepton production in proton-nucleus collisions for energy 5.02 TeV, which are called doubly elastic and single dissociation.

Dilepton production in pA-collisions with a rapidity gap between the nucleus and a high-p_T lepton has been suggested as a probe of the photon partonic content of the proton [3].

Photons as partons of the proton are attracting much attention recently [5–9], as they can play an important role in a number of electroweak processes. They are especially important in event topologies with rapidity gaps as for example in [1,10], but can also have a significant contribution to precise determination of inclusive observables, see, e.g., [11].

II. FORMALISM

Figure 1 shows schematically diagrams of processes included in our present analysis. In the present paper we concentrate on general characteristics and study of differential distribution to select a proper observable for future experimental studies.

*barbarali@dokt.ur.edu.pl
†mluszczak@ur.edu.pl
‡Wolfgang.Schafer@ifj.edu.pl
§antoni.szczurek@ifj.edu.pl

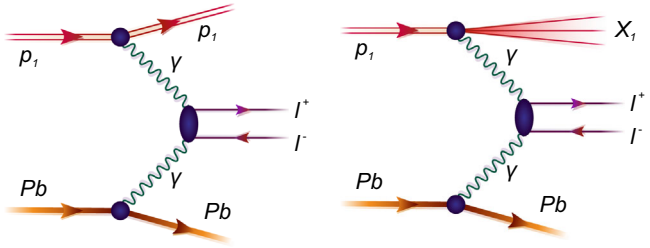

FIG. 1. Classes of processes discussed in the present paper. From left to right: elastic-elastic, inelastic-elastic (or equivalently, elastic-inelastic).

A. Fluxes of elastic photons

To obtain distributions of elastic photons from a proton, it is necessary to express the equivalent photon flux using electric $G_E(Q^2)$ and magnetic $G_M(Q^2)$ form factors, what is expressed as

$$Q^2\frac{d\gamma_{el}^{p}(x,Q^2)}{dQ^2}=\frac{\alpha_{\rm em}}{\pi}\left[\left(1-\frac{x}{2}\right)^2\frac{4m_p^2G_E^2(Q^2)+Q^2G_M^2(Q^2)}{4m_p^2+Q^2}+\frac{x^2}{4}G_M^2(Q^2)\right], \tag{2.1}$$

where x is the fraction of the proton's momentum carried by the photon and m_p is the mass of the proton.

In order to express the elastic photon flux for the nucleus (γ_{el}^{Pb}) in accordance with Ref. [12] we replaced

$$\frac{4m_p^2G_E^2(Q^2)+Q^2G_M^2(Q^2)}{4m_p^2+Q^2}\to Z^2F_{\rm em}^2(Q^2), \tag{2.2}$$

where Z is the charge of the nucleus and $F_{\rm em}(Q^2)$ is its charge form factor.

In the case of the ^{208}Pb nucleus, we used the form factor parametrization used in the STARlight MC generator [13]:

$$F_{\rm em}(Q^2)=\frac{3}{(QR_A)^3}[\sin(QR_A)-QR_A\cos(QR_A)]\frac{1}{1+a^2Q^2}, \tag{2.3}$$

where $Q=\sqrt{Q^2}$, $R_A=1.1A^{1/3}$ fm and $a=0.7$ fm, and $A=208$, $Z=82$.

Integrating the elastic photon parton distribution functions of the proton and the lead nucleus over Q^2 we have

$$\gamma_{el}^{(p,Pb)}(x)=\int_{Q^2_{\rm min}}dQ^2\frac{d\gamma_{el}^{(p,Pb)}(x,Q^2)}{dQ^2},\qquad Q^2_{\rm min}=\frac{x^2m_p^2}{1-x}. \tag{2.4}$$

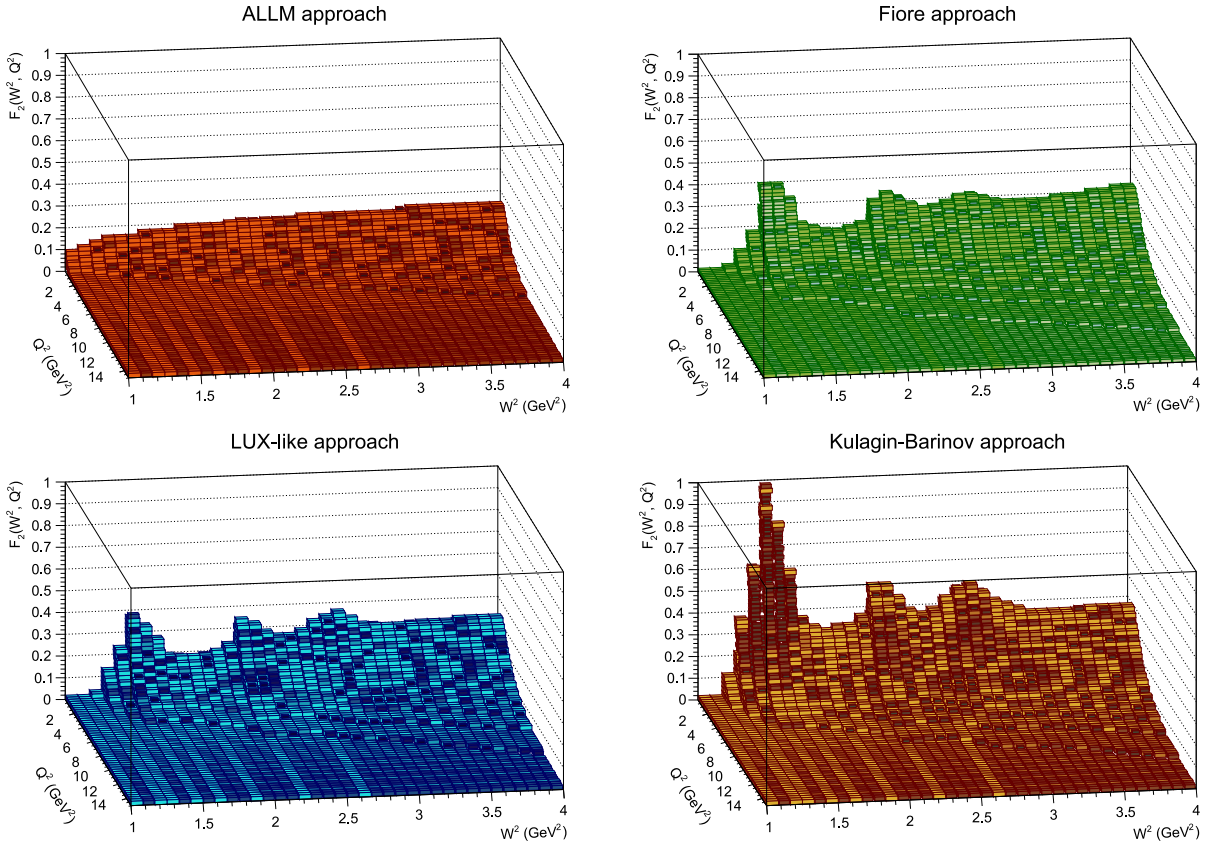

FIG. 2. Different parametrizations of structure functions depending on W^2 and Q^2.

TABLE I. Total cross section for both mass region and different approaches.

Structure function approaches	σ_{LMR} (nb)	σ_{IMR} (nb)
Elastic	2938.72	507.04
LUX-like	346.53	191.40
Kulagin—Barinov	387.93	205.27
Fiore	653.07	347.08
ALLM	329.72	179.07

B. High-energy factorization

In this paper, the k_T-factorization approach, called also high-energy factorization, is used, in which the vertices $\gamma^* p \to X$ can be parameterized in terms of the proton structure function. Photons from inelastic cases are characterized in this approach by having transverse momenta and nonzero virtuality, and by using unintegrated photon distributions. These fluxes, in the deep inelastic scattering limit, can be calculated from the equation (see, e.g., [5,14]):

$$Q^2 \frac{d\gamma^p_{inel}(x,Q^2)}{dQ^2} = \frac{1}{x}\int_{M^2_{\rm thr}} dM_X^2 \mathcal{F}^{\rm in}_{\gamma^*\leftarrow p}(x,\vec{q}_T^{\,2},M_X^2), \tag{2.5}$$

using functions $\mathcal{F}^{\rm in}_{\gamma^*\leftarrow p}$ from [9,12]:

$$\begin{aligned}\mathcal{F}^{\rm in}_{\gamma^*\leftarrow p}&(x,\vec{q}_T^{\,2},M_X)\\ =&\frac{\alpha_{\rm em}}{\pi}\left\{(1-x)\left(\frac{\vec{q}_T^{\,2}}{\vec{q}_T^{\,2}+x(M_X^2-m_p^2)+x^2m_p^2}\right)^2\frac{F_2(x_{\rm Bj},Q^2)}{Q^2+M_X^2-m_p^2}\right.\\ &\left.+\frac{x^2}{4x_{\rm Bj}^2}\frac{\vec{q}_T^{\,2}}{\vec{q}_T^{\,2}+x(M_X^2-m_p^2)+x^2m_p^2}\frac{2x_{\rm Bj}F_1(x_{\rm Bj},Q^2)}{Q^2+M_X^2-m_p^2}\right\},\end{aligned} \tag{2.6}$$

where

$$Q^2 = \frac{\vec{q}_T^{\,2}+x(M_X^2-m_p^2)+x^2m_p^2}{(1-x)}, \tag{2.7}$$

and

$$x_{\rm Bj} = \frac{Q^2}{Q^2+M_X^2-m_p^2}. \tag{2.8}$$

In practice, we use the functions $F_L(x_{\rm Bj},Q^2)$ and $F_2(x_{\rm Bj},Q^2)$ instead of $F_1(x_{\rm Bj},Q^2)$ and $F_2(x_{\rm Bj},Q^2)$. The $F_L(x_{\rm Bj},Q^2)$ function, which is the proton's longitudinal structure function, can be expressed by the functions $F_1(x_{\rm Bj},Q^2)$ and $F_2(x_{\rm Bj},Q^2)$ as:

$$F_L(x_{\rm Bj},Q^2) = \left(1+\frac{4x_{\rm Bj}^2m_p^2}{Q^2}\right)F_2(x_{\rm Bj},Q^2) - 2x_{\rm Bj}F_1(x_{\rm Bj},Q^2). \tag{2.9}$$

Therefore, in the k_T-factorization approach, the cross-section for the $p+Pb\to Pb+l^+l^-+X$ processes is (taking into account unintegrated photon flux):

$$\begin{aligned}\sigma = S^2\int dx_p dx_{\rm Pb}\frac{d^2\vec{q}_T}{\pi}&\left[\frac{d\gamma^p_{el}(x_p,Q^2)}{dQ^2}+\frac{d\gamma^p_{inel}(x_p,Q^2)}{dQ^2}\right]\\ &\times\gamma^{\rm Pb}_{el}(x_{\rm Pb})\sigma_{\gamma^*\gamma\to\ell^+\ell^-}(x_p,x_{\rm Pb},\vec{q}_T),\end{aligned} \tag{2.10}$$

where $\sigma_{\gamma^*\gamma\to\ell^+\ell^-}$ is the off-shell elementary cross-section (for details see Refs. [14,15]) and for $x_p \ll 1$ we can assume that $Q^2 \approx \vec{q}_T^{\,2}$ [see Eq. (2.7)].

Here we also put a gap-survival factor $S^2 \le 1$ in front. In fact the gap survival probability is expected to depend on the kinematics of the process. It should be applied when asking for a rapidity gap. The modeling of the latter goes beyond the scope of this work. Furthermore, we concentrate on the contribution to inclusive observables, where $S^2 = 1$.

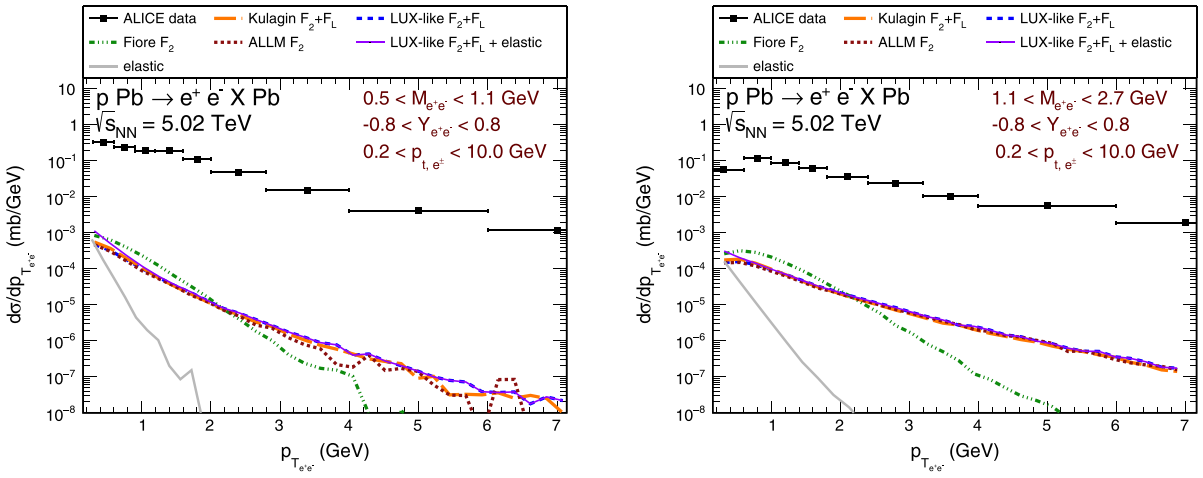

FIG. 3. Distributions in $p_{T_{e^+e^-}}$ for LMR on the left and for the IMR on the right.

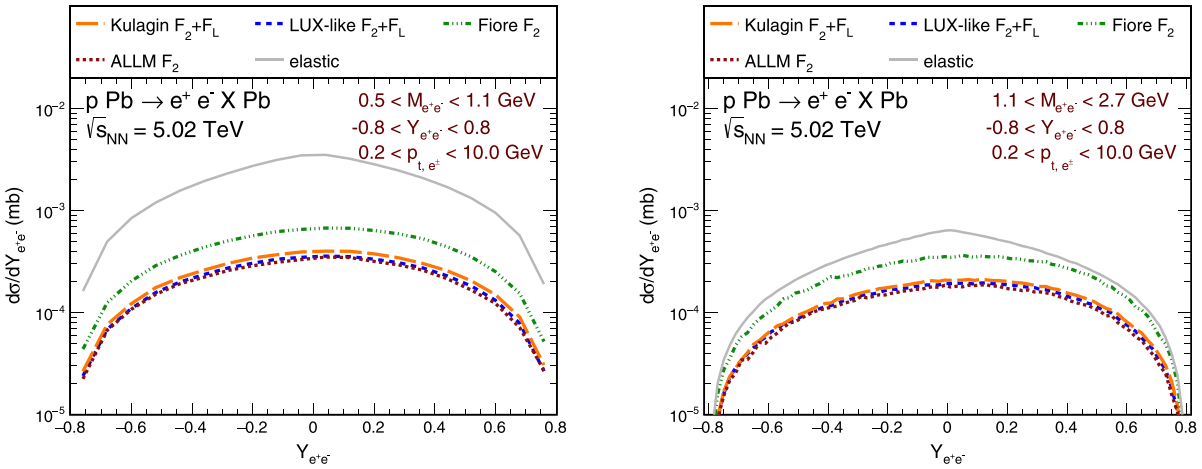

FIG. 4. Distributions in $Y_{e^+e^-}$ for LMR on the left and for the IMR on the right.

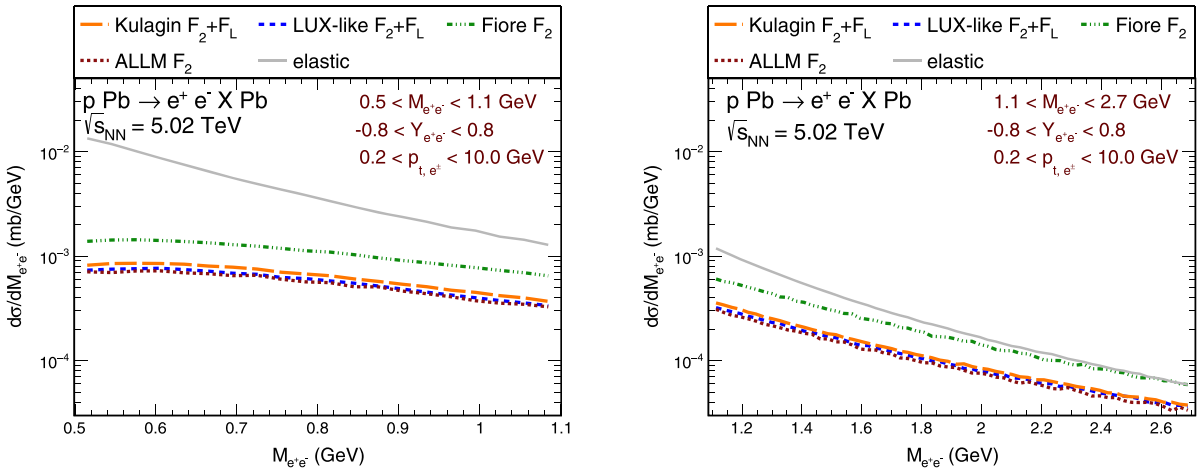

FIG. 5. Distributions in $M_{e^+e^-}$ for LMR on the left and for the IMR on the right.

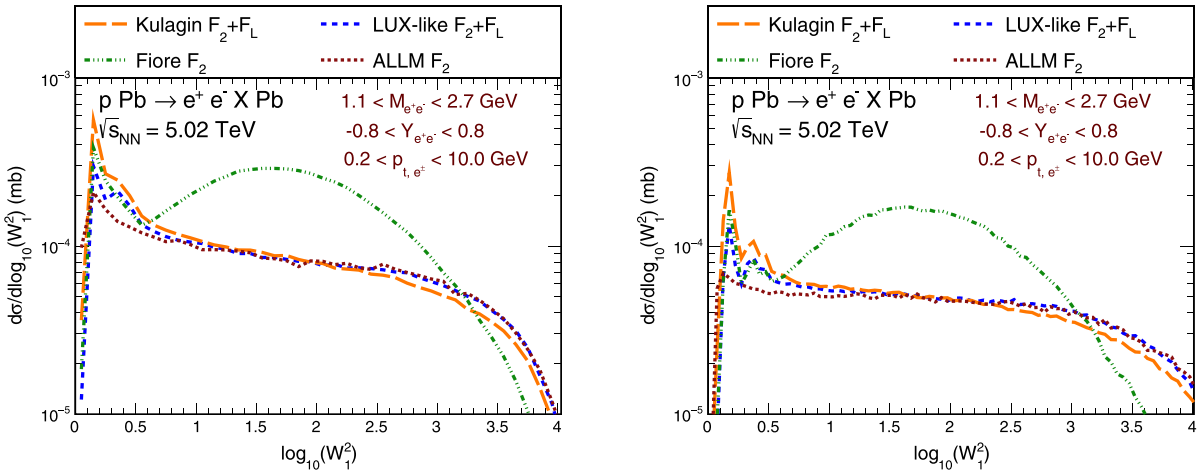

FIG. 6. Distribution in $\log(W^2)$ for LMR on the left and for the IMR on the right.

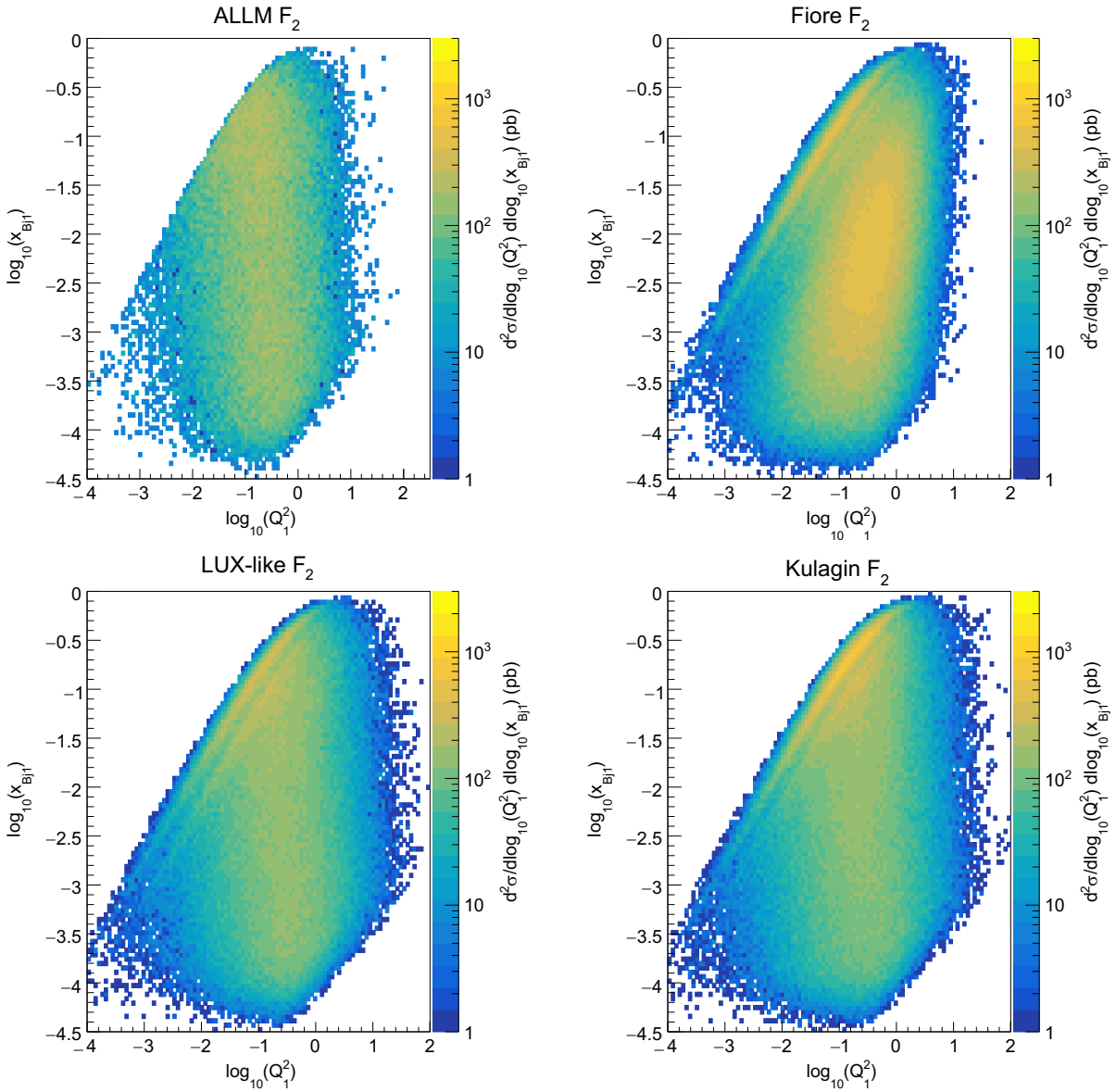

FIG. 7. Distribution in $\log_{10} x_{Bj}$ and $\log_{10} Q^2$ for four approaches of structure function: ALLM, Fiore, LUX-like, and Kulagin, respectively for LMR.

Importantly, despite the fact that the fluxes do not depend on the $\vec{q}_T$ direction, for collinear case, the averaging over $\vec{q}_T$ directions in the off-shell cross-sections replaces the average of photon polarization.

C. Structure function parametrizations

We expect, that in the kinematical region of interest in this work, the main contribution will come from the structure functions probed in the nonperturbative region, where their Q^2 and x_{Bj} dependence cannot be calculated by perturbative QCD. To control the inevitable model dependence, we use a variety of structure function parametrizations. Three of them, the ALLM [16,17], FFJLM (Fiore *et al.*) [18] and LUX-like [19] were already used in our previous publications and are described in more detail in Ref. [9]. A new addition in this work is a parametrization by Kulagin and Barinov [20].

In Fig. 2 we show the four different parametrizations of the structure function F_2 of the proton in the (W^2, Q^2)-plane. Here

$$W^2 = \frac{1 - x_{\mathrm{Bj}}}{x_{\mathrm{Bj}}} Q^2 + m_p^2 \tag{2.11}$$

is the $\gamma^* p$ cm-energy squared, so that W is the invariant mass of the hadronic final state.

Here we observe, that the ALLM parametrization does not show the prominent resonance structures at low invariant mass. Indeed it is constructed in the spirit of

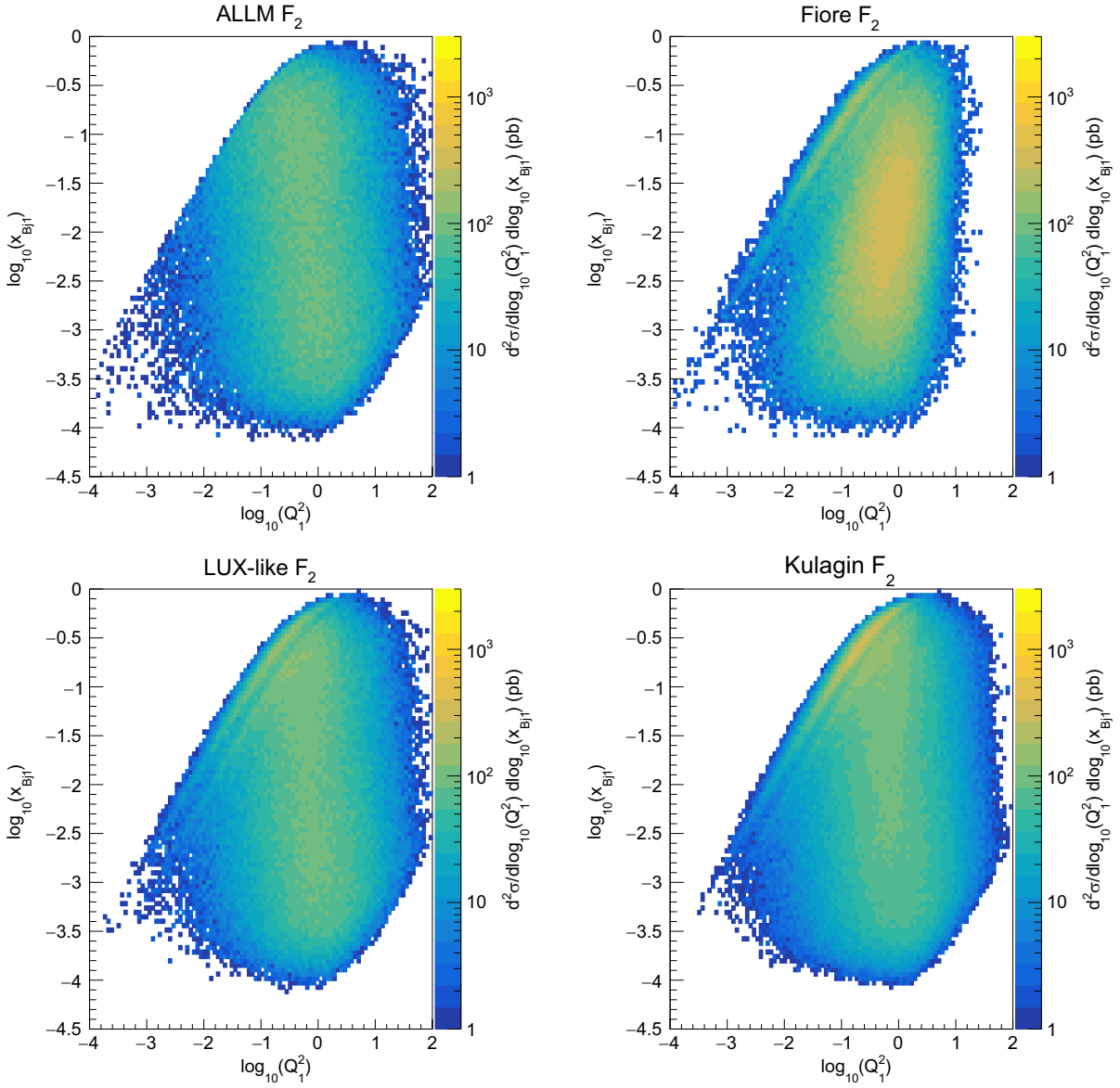

FIG. 8. Distribution in $\log x_{\mathrm{Bj}}$ and $\log Q^2$ for four approaches of structure function: ALLM, Fiore, LUX-like, and Kulagin, respectively for IMR.

parton-hadron duality and represents rather an "averaged" F_2. The remaining three parametrizations all contain explicit resonances, which are especially visible at low Q^2.

III. RESULTS

In Table I we show integrated cross sections for different categories of $\gamma\gamma$ processes shown in Fig. 1 for two different mass regions corresponding to the ALICE Collaboration results: low-mass region (LMR), where $0.5 < M_{ee} < 1.1$ GeV and intermediate-mass region (IMR) for $1.1 < M_{ee} < 2.7$ GeV.

Cross sections as a function of some variables are presented separately for two different mass regions corresponding to the ALICE Collaboration regions: low-mass region (LMR) and intermediate-mass region (IMR).

The elastic contribution gives much larger contribution, especially for LMR. The ALLM, LUX-like and Kulagin-Barinov parametrization, although differing in some regions of the (x_{Bj}, Q^2) space give similar predictions for the integrated cross section.

Distributions in transverse momenta (see Fig. 3) correspond to the ALICE inclusive data. The $\gamma\gamma$ contribution is calculated here for the first time. It is much smaller than experimental ALICE data and contributions of other mechanism of dilepton production discussed, e.g., in [4].

Imposing an extra condition on rapidity gap one can select the $\gamma\gamma$ mechanism. Now we will concentrate therefore only on the $\gamma\gamma$ fusion. One can observe that the elastic contribution dominates at low lepton pair transverse momenta. The region of larger transverse momenta $p_{T,ee} > 1$ GeV is dominated

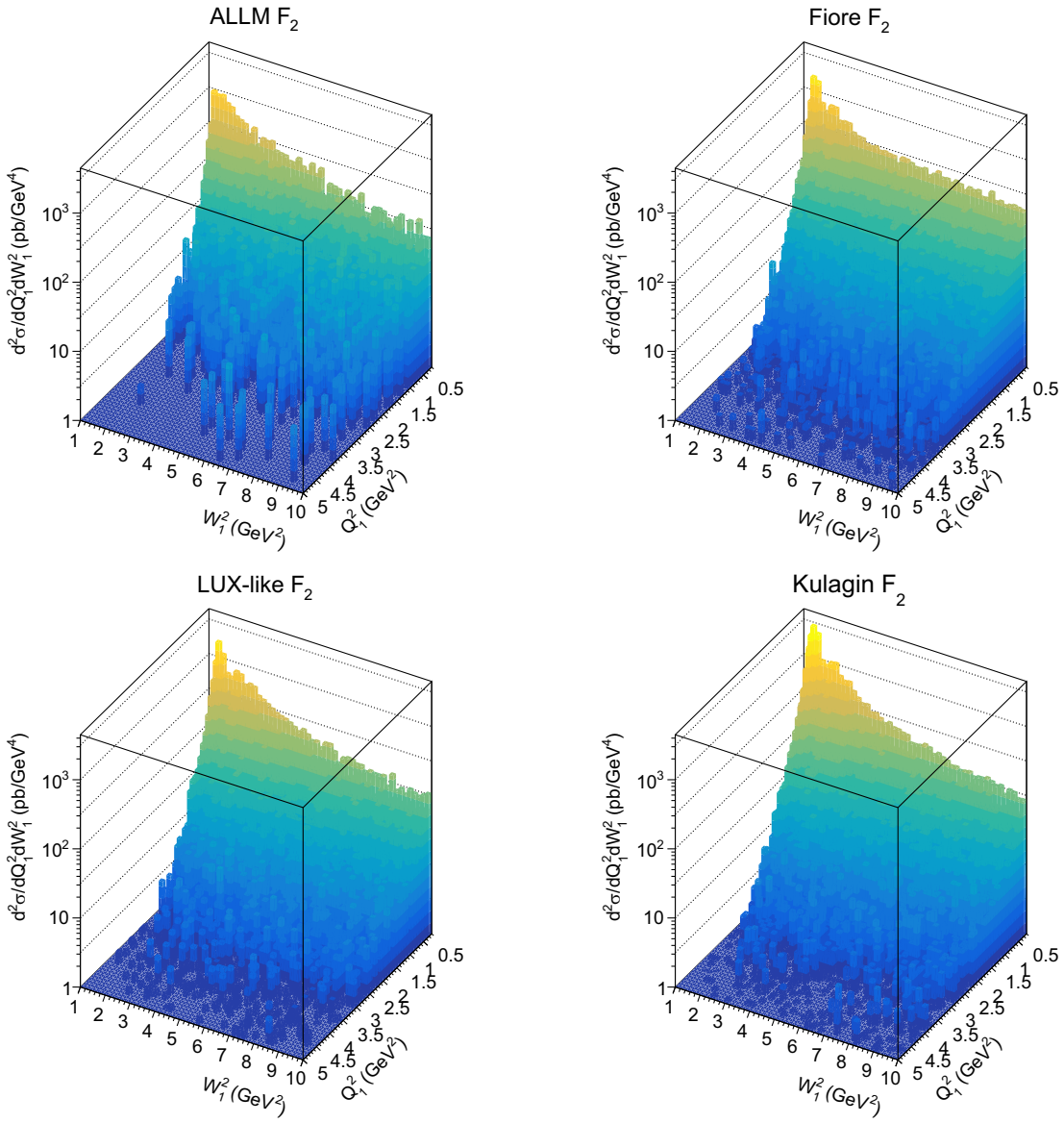

FIG. 9. Distribution in W^2 and Q^2 for four approaches of structure function: ALLM, Fiore, LUX-like, and Kulagin, respectively for LMR.

by the inelastic contribution. The differences for different parametrizations become visible for $p_{T,ee} > 3$ GeV, where the cross section is rather small. It is not clear to us whether such a study will be possible within run 3 or run 4 of the LHC.

The distributions in pair rapidity (within ALICE acceptance) are shown in Fig. 4. Here the three structure function parametrizations give very similar distributions.

In Fig. 5 we show the dielectron invariant mass distribution for the elastic-elastic and inelastic-elastic contributions. The first one gives a larger contribution than the second one. All structure functions, except of Fiore *et al.* [18] give very similar distributions which gives confidence in our calculation.

It is also interesting to inspect the rather theoretical distribution in photon-proton energy W_1. In Fig. 6 we show distributions rather in $\log_{10} W_1^2$, where $W_1^2 = \frac{Q_1^2}{x_{Bj_1}} - Q_1^2 + m_p^2$, in order to cover the whole energy interval on one plot. Again the Fiore *et al.* parametrization [18] gives quite different distribution. The results of other parametrization differ in the region of low W_1 where proton resonances occur. However, as discussed before, their contribution is not crucial for the distributions in $Y_{e^+e^-}$ or $M_{e^+e^-}$.

Now we shall look more differentially. It is interesting to understand what regions of arguments of structure functions are important for the two-photon dilepton production. We start form the $(\log_{10} Q^2, \log_{10} x_{\mathrm{Bj}})$ distributions (see Figs. 7 and 8). The figures show that our selected measurement with its specific cuts covers rather broad

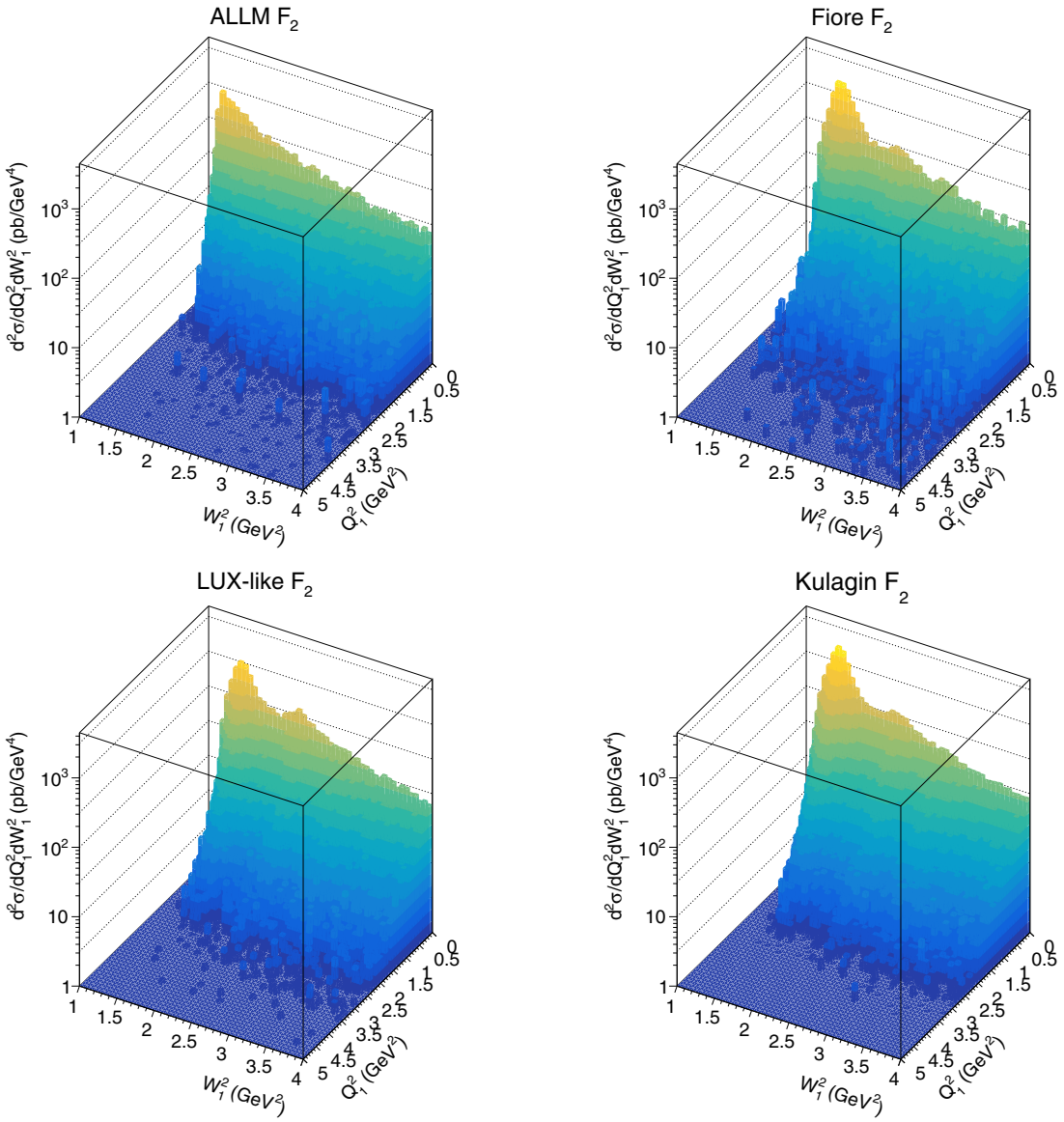

FIG. 10. Distribution in $\log_{10} W^2$ and $\log_{10} Q^2$ for four approaches of structure function: ALLM, Fiore, LUX-like, and Kulagin, respectively for IMR.

range of x_{Bj}. A big part of the cross section comes from $Q_1^2 < 1$ GeV^2, i.e., from clearly nonperturbative region, where partonic description breaks.

Finally for completeness in Figs. 9 and 10 we present also $(\log_{10} W_1^2, \log_{10} Q^2)$ distributions limiting to small range of W_1. Except for the ALLM parametrization, we clearly see contributions of individual resonances. We observe rather slight differences for different parametrizations.

IV. RAPIDITY GAPS

Our calculation in this paper was done in the momentum space. It is not clear how big are corrections related to destroying rapidity gaps. For $AA \to AAl^+l^-$ reaction such corrections are usually calculated in the impact parameter space by imposing geometrical conditions [e.g., $\theta(b - R_1 - R_2)$] in the multidimensional integral [13,21]. For $p + A$ collisions one can do the same. In the following we shall follow this method using the SuperChic program [22–24]. We are particularly interested to which extent the geometrical conditions change the dilepton invariant mass distribution. In Table II we show such numbers for different windows of invariant mass: (0–5) GeV, (5–10) GeV, (10–15) GeV, and (15–20) GeV. We see that the absorption effects due to $p + {}^{208}Pb$ collisions lead to damping the cross section. For low invariant masses $M \in (0\text{–}5)$ GeV the damping factor—the gap survival factor is 0.95, so the modification is rather small.

There is also an interesting experimental aspect how to assure the $p + {}^{208}$Pb UPC. When talking about ALICE

TABLE II. Total cross section from SuperChic program for different bins of masses from 0 to 20 GeV with corresponding gap survival factor S_G.

Mass region	0.5–5 (GeV)	5–10 (GeV)	10–15 (GeV)	15–20 (GeV)
No soft S_G	755.91 (nb)	687.74 (nb)	98.68 (nb)	28.23 (nb)
With soft S_G	718.84 (nb)	623.27 (nb)	87.01 (nb)	24.33 (nb)
$\langle S_G \rangle$	0.95	0.91	0.88	0.86

apparatus one can use the zero degree calorimeter and impose a condition of no neutrons in the direction of nucleus. For the asymmetric $p + {}^{208}Pb$ collisions neutrons can be emitted when the proton collides with the lead nucleus. In this case the probability of Coulomb excitation in UPC is very small. One could also look at neutrons on the proton side. In principle, also protons can be measured in forward directions [25–27]. According to our knowledge this option was not used so far. One could also use standard methods applied for ${}^{208}Pb + {}^{208}Pb \to e^+e^-$ UPC [28], including VZERO detectors with requirement of no signal and small number of reconstructed tracks in TPC.

V. CONCLUSIONS

In the present paper we have calculated the photon-photon contribution to the inclusive e^+e^- pair production in proton-Pb collisions. We have included processes when the proton survives (elastic case) and when the proton dissociates (inelastic case). The calculations have been performed in the so-called k_t-factorization approach including transverse momenta of intermediate photons. Modern parametrizations of proton structure functions have been used in the calculation.

The results have been compared to the existing data (distributions in transverse momentum of the dielectron pair) measured by the ALICE collaboration for two different windows on dielectron invariant mass, LMR ($0.5 < M_{ee} < 1.1$ GeV) and IMR ($1.1 < M_{ee} < 2.7$ GeV). We have checked that such a contribution is more than two orders of magnitude smaller than the published ALICE data. We conclude that the two-photon mechanism gives negligible contribution to the inclusive cross section.

The two-photon processes are interesting by themselves and could be studied in the future. This can be done by imposing rapidity gap veto.

We have calculated the distributions in transverse momentum of the dilepton pair for different modern parametrizations of proton structure functions. We have shown that the region of relatively low dielectron masses (LMR + IMR) is sensitive to the nonperturbative regions (low-Q^2), and a broad range of Bjorken-x. We have presented two-dimensional distributions in these variables ($\log_{10} Q^2, \log_{10} x_{Bj}$) and also in ($Q^2$, W^2). The second set of two-dimensional distributions shows that the ALICE kinematics could test also the region of nucleon resonances, and actually a sizeable contribution to the distributions come from this region. The different parametrizations used by us (Fiore *et al.*, ALLM, Lux-like, and Kulagin *et al.*) treat somewhat differently this domain of the structure functions. The Fiore *et al.* parametrization gives a quite different result than the other used parametrizations. However, the Fiore parametrization was obtained from a fit to a rather narrow range of Q^2 and W relevant for JLAB kinematics only. Extending this fit outside the JLAB region may be not justified.

We have estimated the gap survival factor using the impact parameter space calculation. The gap survival factor found depends on the dielectron invariant mass but decreases the cross section by only 5%–10%.

We finally wish to mention that there are other corrections which are only partially captured by the gap survival factor, and which are related to QED corrections and are enhanced by $(Z\alpha)^n$. These corrections break the factorization ansatz adopted in this work. First, there are unitarity QED corrections related to the production of multiple pairs [29]. Second, there are multiple photon exchanges between the ion and the lepton pair, see, e.g., [30,31]. These corrections are expected to be important if the relative transverse momenta of leptons is very small, i.e., when the dilepton pair form a large electric dipole in impact parameter space. They must be addressed, if experimental data of sufficient accuracy will become available in the future.

ACKNOWLEDGMENTS

This study was partially supported by the Polish National Science Center Grant No. UMO-2018/31/B/ST2/03537 and by the Center for Innovation and Transfer of Natural Sciences and Engineering Knowledge in Rzeszow. We thank Rainer Schicker and Adam Matyja for a discussion of the ALICE apparatus.

[1] L. Forthomme, M. Łuszczak, W. Schäfer, and A. Szczurek, Phys. Lett. B **789**, 300 (2019).
[2] M. Kłusek-Gawenda, R. Rapp, W. Schäfer, and A. Szczurek, Phys. Lett. B **790**, 339 (2019).
[3] M. Dyndal, A. Glazov, M. Luszczak, and R. Sadykov, Phys. Rev. D **99**, 114008 (2019).
[4] S. Acharya *et al.* (ALICE Collaboration), Phys. Rev. C **102**, 055204 (2020).
[5] M. Luszczak, W. Schäfer, and A. Szczurek, Phys. Rev. D **93**, 074018 (2016).
[6] A. Manohar, P. Nason, G. P. Salam, and G. Zanderighi, Phys. Rev. Lett. **117**, 242002 (2016).
[7] F. Giuli *et al.* (xFitter Developers' Team Collaboration), Eur. Phys. J. C **77**, 400 (2017).
[8] L. Harland-Lang, A. Martin, R. Nathvani, and R. Thorne, Eur. Phys. J. C **79**, 811 (2019).
[9] M. Łuszczak, W. Schäfer, and A. Szczurek, J. High Energy Phys. 05 (2018) 064.
[10] M. Łuszczak, L. Forthomme, W. Schäfer, and A. Szczurek, J. High Energy Phys. 02 (2019) 100.
[11] A. Denner and S. Dittmaier, Phys. Rep. **864**, 1 (2020).
[12] V. M. Budnev, I. F. Ginzburg, G. V. Meledin, and V. G. Serbo, Phys. Rep. **15**, 181 (1975).
[13] S. R. Klein, J. Nystrand, J. Seger, Y. Gorbunov, and J. Butterworth, Comput. Phys. Commun. **212**, 258 (2017).
[14] G. G. da Silveira, L. Forthomme, K. Piotrzkowski, W. Schäfer, and A. Szczurek, J. High Energy Phys. 02 (2015) 159.
[15] S. Catani, M. Ciafaloni, and F. Hautmann, Nucl. Phys. **B366**, 135 (1991).
[16] H. Abramowicz, E. M. Levin, A. Levy, and U. Maor, Phys. Lett. B **269**, 465 (1991).
[17] H. Abramowicz and A. Levy, arXiv:hep-ph/9712415.
[18] R. Fiore, A. Flachi, L. Jenkovszky, A. Lengyel, and V. Magas, Eur. Phys. J. A **15**, 505 (2002).
[19] A. V. Manohar, P. Nason, G. P. Salam, and G. Zanderighi, J. High Energy Phys. 12 (2017) 046.
[20] S. A. Kulagin and V. V. Barinov, Phys. Rev. C **105**, 045204 (2022).
[21] A. van Hameren, M. Kłusek-Gawenda, and A. Szczurek, Phys. Lett. B **776**, 84 (2018).
[22] L. A. Harland-Lang, M. Tasevsky, V. A. Khoze, and M. G. Ryskin, Eur. Phys. J. C **80**, 925 (2020).
[23] L. A. Harland-Lang, V. A. Khoze, M. G. Ryskin, and W. J. Stirling, Eur. Phys. J. C **69**, 179 (2010).
[24] L. A. Harland-Lang, V. A. Khoze, M. G. Ryskin, and W. J. Stirling, Eur. Phys. J. C **72**, 2110 (2012).
[25] R. Gemme *et al.*, Nucl. Phys. B, Proc. Suppl. **197**, 211 (2009).
[26] C. Oppedisano *et al.*, Nucl. Phys. B, Proc. Suppl. **197**, 206 (2009).
[27] G. Puddu *et al.*, Nucl. Instrum. Methods Phys. Res., Sect. A **604**, 765 (2009).
[28] E. Abbas *et al.* (ALICE Collaboration), Eur. Phys. J. C **73**, 2617 (2013).
[29] U. D. Jentschura, K. Hencken, and V. G. Serbo, Eur. Phys. J. C **58**, 281 (2008).
[30] E. Bartos, S. R. Gevorkyan, E. A. Kuraev, and N. N. Nikolaev, Phys. Rev. A **66**, 042720 (2002).
[31] D. Ivanov and K. Melnikov, Phys. Rev. D **57**, 4025 (1998).